Acta Astronautica ▮ (▮▮▮▮) ▮▮▮–▮▮▮

Contents lists available at ScienceDirect

Acta Astronautica

journal homepage: www.elsevier.com/locate/actaastro

Flat-spin recovery of spinning satellites by an equatorial torque

Frank L. Janssens [a], Jozef C. van der Ha [b,*]

[a] Wilhelminastraat 29, 2201 KA Noordwijk, The Netherlands
[b] 5808 Bell Creek Road, Deming, WA 98244, USA

ARTICLE INFO

Article history:
Received 23 June 2014
Received in revised form
18 February 2015
Accepted 5 May 2015

Keywords:
Spinning satellites
Attitude dynamics
Flat-spin recovery

ABSTRACT

The recovery from a flat-spin motion represents one of the most impressive practical applications in the field of spinning-satellite dynamics. The present paper presents flat-spin recovery maneuvers by means of a body-fixed torque within the plane perpendicular to the maximum principal axis of inertia. The conditions for a successful recovery are established. These are quite different from those obtained in the case when the torque is along the minimum axis of inertia where a minimum torque level is required for a successful recovery. If the torque component along the intermediate axis is negative, a recovery from a pure flat spin can be established for any torque magnitude. However, the time to recovery increases indefinitely when this torque component approaches zero. During the recovery maneuver, the angular velocity and angular momentum vectors become aligned with the minimum axis of inertia by turning over about 90° in the body frame. In inertial space, however, the angular momentum stays in the vicinity of its orientation before the start of the recovery.

1. Introduction

The problem of flat-spin recovery made its appearance when spinning satellites had to perform orbit injection maneuvers into their final mission orbit or trajectory after having been launched in a transfer or parking orbit. Therefore, spacecraft were equipped with a rocket motor and in most cases the spacecraft-motor configuration became prolate. Hence, it was spinning about the minimum axis of inertia. In the presence of dissipation (e.g., fuel slosh, vibrations) and in the absence of an active stabilization mechanism, the spacecraft would reorient itself and end up spinning about its maximum axis of inertia as illustrated in Fig. 1. We call this state '*pure flat spin*' or '*flat spin*' depending on the presence of nutation about the maximum axis. The re-establishment of a spin about the minimum axis is called '*flat-spin recovery*'.

One of the first papers about flat-spin recovery is by Barba et al. [1] (1973) and focuses on the SMS meteorological satellite. In the first part, a recovery procedure using a pure spin-up torque about the minimum axis is analyzed. For an asymmetric satellite they find that the torque must exceed a critical value to make the recovery possible. However, their derivation of the critical value uses the assumption of a symmetrical satellite. As a consequence, their critical value is unfortunately too low for an asymmetric satellite. Also they develop a recovery procedure using the available thrusters on SMS. The analysis is done by numerical simulations and illustrates very well the practical implementation of a recovery.

The model they use is a special case of the mathematical problem known as the self-excited rigid body (SERB) [2–5].

* Corresponding author.
E-mail addresses: f.janssens@ziggo.nl (F.L. Janssens), jvdha@aol.com (J.C. van der Ha).

http://dx.doi.org/10.1016/j.actaastro.2015.05.011
0094-5765/

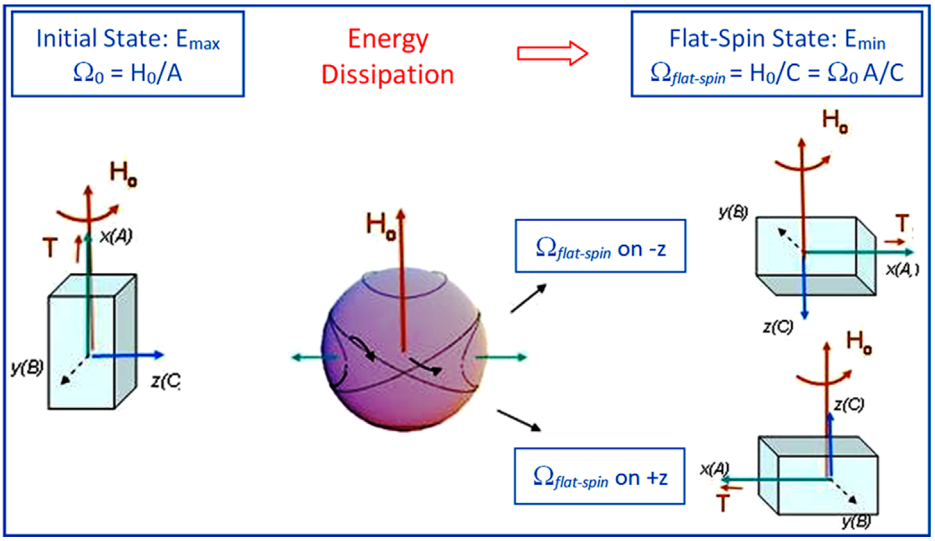

Fig. 1. Visualization of possible flat-spin attitude sequences.

This field of research deals with the dynamics of a spinning body subject to a torque with constant components in the body's coordinate frame. Progress in mathematical methods in this field can be useful for the design of efficient recovery procedures and other satellite dynamics applications as shown more recently by Longuski and Tsiotras [6].

Cronin (1978) [7] derives the correct value for the critical torque about the minimum axis of inertia of an asymmetric body for initial conditions of a pure flat-spin. Livneh and Wie [8,9] find the same result in modern terminology together with a complete discussion of torques on any of the principal axes.

As illustrated in Fig. 1, a transition into a flat spin may result in a positive or negative spin about the major axis of inertia. Rahn and Barba [10] show how the desired orientation of a spacecraft entering into a flat-spin can be achieved by two thruster impulses.

Recovery procedures based on a torque motor, as opposed to thrusters, have also been investigated [11,12]. In these cases, the SERB model is replaced by the dual-spin dynamical model.

In a previous paper [13] we present analytical results for the flat-spin recovery under a body-fixed torque pointing along the minor principal axis for arbitrary initial nutation conditions. We derive a solution in the form of a generalized pendulum equation for the increasing angular velocity along the torque axis in the body frame. Thus, the motion is similar to that of a pendulum which is either oscillating (no recovery) or revolving (recovery) with increasing angular velocity. The minimum torque level that guarantees a flat-spin recovery occurs precisely at the transition between these two cases. Also we found that the minimum required torque level for a recovery depends on the nutation phase angle. Approximate analytical results show the motion in inertial coordinates.

The pendulum-type solution follows from the existence of two first integrals. The first integration constant states that the amplitude of the rotational motion in the plane perpendicular to the torque remains constant. Ref. [13] presents explicit results for the decrease in the nutation angle after the recovery.

In this paper, we consider bodies with three different moments of inertia subjected to a more general torque acting within the plane normal the maximum inertia axis. In this case, only one first integral is available and no pendulum-like solution can be constructed. Thus, we study here only recovery strategies that start from a *pure* flat-spin situation, i.e. in the absence of nutation.

In the present case, the transition to the flat-spin recovery does not need to happen in the first revolution as was the case for a torque about the minimum-inertia axis in Ref. [13]. When the torque component on the intermediate axis is negative, the angular velocity along the major axis shows a secular decrease and the transition to a rotation about the minimum inertia axis will occur eventually. For a given torque magnitude, we can establish the optimum orientation of the torque that minimizes the time until the transition.

2. Dynamical equations of motion

The motion of an asymmetric rigid body under a constant body-fixed torque is described by the Euler equations [14]:

$$A\dot{\omega}_1+(C-B)\omega_2\omega_3=T_1 \tag{1a}$$

$$B\dot{\omega}_2-(C-A)\omega_1\omega_3=T_2 \tag{1b}$$

$$C\dot{\omega}_3+(B-A)\omega_1\omega_2=T_3 \tag{1c}$$

Here, the dot denotes the time-derivative, ω_j are the components of the rotation vector $\boldsymbol{\omega}$. The subscripts $j=1$, 2, 3 refer to the x, y, z principal body axes that are associated with the principal moments of inertia A, B, and C, respectively, and satisfy the following sequence:

$$A<B<C \tag{2}$$

Please cite this article as: F.L. Janssens, J.C. van der Ha, Flat-spin recovery of spinning satellites by an equatorial torque, Acta Astronautica (2015), http://dx.doi.org/10.1016/j.actaastro.2015.05.011

The torque vector **T** has components T_j along the principal axes, see Eqs. (1a)–(1c). We consider here the specific case when $T_1 > 0$, T_2 may have either sign, and T_3 vanishes. In the presence of torques, the rotational energy E and the modulus of the angular momentum vector $H = |\mathbf{H}|$ are the same physical quantities as in the torque-free case but become functions of time t:

$$E(t) = \frac{1}{2}\{A\omega_1^2 + B\omega_2^2 + C\omega_3^2\} \tag{3a}$$

$$H^2(t) = \left\{A^2\omega_1^2 + B^2\omega_2^2 + C^2\omega_3^2\right\} \tag{3b}$$

In the presence of an arbitrary torque vector **T**, it follows from Eqs. (1a)–(1c) that the rates of change of the rotational energy E and the angular-momentum-squared H^2 are given by

$$\frac{d}{dt}(E) = \boldsymbol{\omega} \bullet \mathbf{T}; \quad \frac{d}{dt}\left(H^2\right) = 2(\mathbf{H} \bullet \mathbf{T}) \tag{4a, b}$$

Thus, the energy remains unchanged if the torque vector acts perpendicular to the rotation vector. Likewise, the modulus of the angular momentum vector remains constant if the torque vector acts perpendicular to the angular momentum vector.

From the definitions of $E(t)$, $H(t)$ and the conditions stated in Eq. (2) we find that, for a given value $H(t)$, the corresponding energy $E(t)$ lies within the range:

$$E_{min}(t) = \frac{H^2(t)}{2C} < E(t) < \frac{H^2(t)}{2A} = E_{max}(t) \tag{5}$$

The range of energy values in Eq. (5) can be separated in two intervals as visualized in Fig. 2. We define the motion to be spinning about

$$(a)\ z-axis,\ if: \quad E_{min}(t) < E(t) < \frac{H^2(t)}{2B} = E_{sep}(t) \tag{6a}$$

$$(b)\ x-axis,\ if: \quad E_{sep}(t) < E(t) < E_{max}(t) \tag{6b}$$

where 'sep' denotes the separatrix, see Fig. 2.

We consider an arbitrary torque that has been acting during the interval $0 \le \tau \le t$ and terminates at time t. When the instantaneous values $E(t)$ and $H(t)$ satisfy Eq. (6a), we have

$$\Delta E_{sep}(t) = E_{sep}(t) - E(t) = \frac{1}{2B}\{C(C-B)\omega_3^2 - A(B-A)\omega_1^2\} > 0 \tag{7}$$

and the body is still spinning about its major inertia axis z as it does from the start at $\tau = 0$.

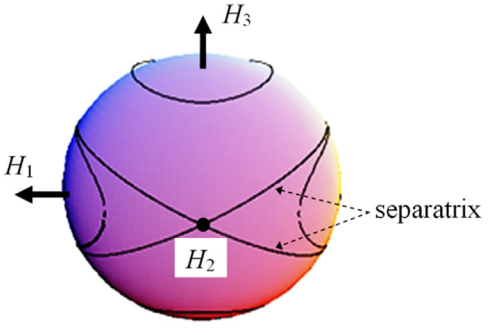

Fig. 2. Constant energy levels on the angular momentum sphere.

On the other hand, if $\Delta E_{sep} < 0$, Eq. (6b) shows that the body is already spinning about its minor inertia axis (x). Thus, the condition $\Delta E_{sep} = 0$ characterizes the transition from a rotation about the maximum inertia (z) to a rotation about the minimum inertia axis (x). Therefore, it is the goal of a recovery maneuver to achieve $\Delta E_{sep} < 0$.

The rate of change of $\Delta E_{sep}(t)$ follows by combining the results of Eq. (7) and Eqs. (4a) and (4b):

$$\begin{aligned}\Delta\dot{E}_{sep}(t) &= \dot{E}_{sep}(t) - \dot{E}(t) = \frac{1}{2B}\frac{d(H^2)}{dt} - \dot{E}(t) \\ &= \left(\frac{\mathbf{H}}{B} - \boldsymbol{\omega}\right) \bullet \mathbf{T} = -\left(\frac{B-A}{B}\right)\omega_1 T_1\end{aligned} \tag{8}$$

Thus, the rate of change of $\Delta E_{sep}(t)$ depends only on the torque component T_1 and not on T_2. Because we assume $T_1 > 0$, $\Delta E_{sep}(t)$ decreases as long as $\omega_1 > 0$. Once the body starts spinning about the minor principal axis, $\omega_1 > 0$ keeps its sign so that a continuing spin-up is guaranteed.

A similar quantity that also plays an important role is the (positive) difference between the maximum possible energy $E_{max} = H^2/(2A)$, which is compatible with the actual instantaneous angular momentum $H(t)$, and the actual instantaneous energy $E(t)$:

$$\Delta E_{max}(t) = \frac{H^2(t)}{2A} - E(t) = \frac{1}{2A}\{B(B-A)\omega_2^2 + C(C-A)\omega_3^2\} \tag{9}$$

Similarly as for ΔE_{sep}, the rate of change of ΔE_{max} can be calculated as follows:

$$\begin{aligned}\Delta\dot{E}_{max}(t) &= \dot{E}_{max}(t) - \dot{E}(t) = \frac{1}{2A}\frac{d(H^2)}{dt} - \dot{E}(t) \\ &= \left(\frac{\mathbf{H}}{A} - \boldsymbol{\omega}\right) \bullet \mathbf{T} = \left(\frac{B-A}{A}\right)\omega_2 T_2\end{aligned} \tag{10}$$

Thus, the rate of change of $\Delta E_{max}(t)$ depends only on the torque component T_2.

3. Torque about minimum axis of inertia

The case when the torque component $T_1 \neq 0$ (and $T_2 = T_3 = 0$) was investigated in a previous paper [13] by the authors. Here, we follow a different approach that facilitates the comparison with the present model where both T_1 and $T_2 \neq 0$ and with its results that turn out to be very different.

When $T_2 = 0$, Eq. (10) shows that the quantity ΔE_{max}, which is a particular *linear combination of the rotational energy and the* (*modulus of the*) *angular momentum*, *remains constant*. Thus, $\Delta E_{max}(t) = \Delta E_{max}(0) = \Delta E_0$ is a first integral of the system in Eqs. (1a)–(1c) in this case.

Eq. (9) indicates that the projection of the angular velocity vector on the y, z-plane describes an ellipse with constant semi-major axis a on the y-axis and semi-minor axis b on the z-axis:

$$a = \sqrt{\frac{2A\,\Delta E_0}{B(B-A)}} > b = \sqrt{\frac{2A\,\Delta E_0}{C(C-A)}} \tag{11a, b}$$

The parametric equations of this ellipse and its derivatives are given by

$$\omega_2(t) = a\ \cos u(t); \quad \omega_3(t) = b\ \sin u(t) \tag{12a, b}$$

Please cite this article as: F.L. Janssens, J.C. van der Ha, Flat-spin recovery of spinning satellites by an equatorial torque, Acta Astronautica (2015), http://dx.doi.org/10.1016/j.actaastro.2015.05.011

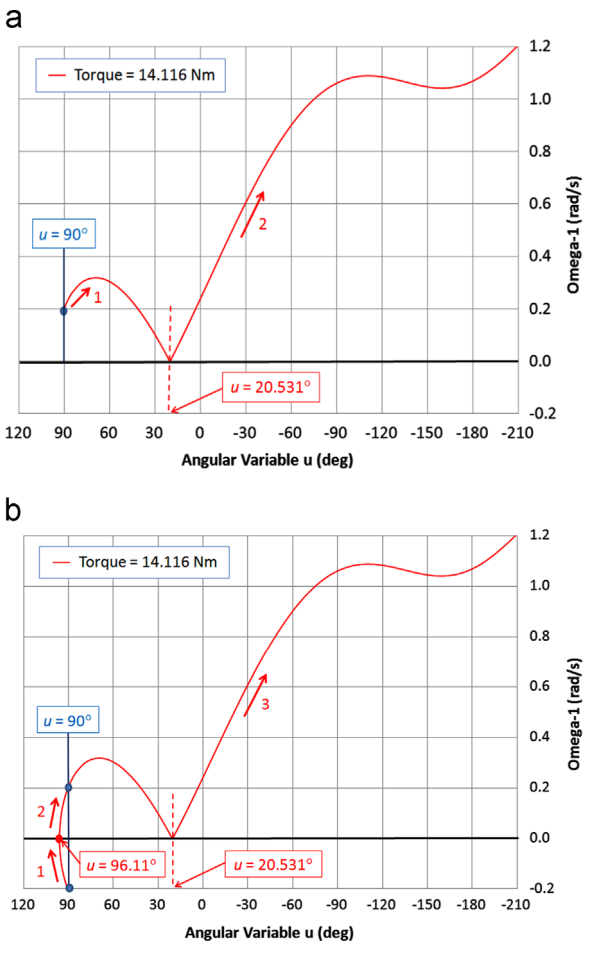

Fig. 3. (a) Evolution of $\omega_1(u)$ for case $\omega_{10}>0$. (Inputs: $A=200$; $B=300$; $C=400$ kg m^2; $\omega_{10}=2.070$; $\omega_{20}=0$; $\omega_{30}=5$ rpm). (b) Evolution of $\omega_1(u)$ for case $\omega_{10}<0$. (Inputs as in Fig. 3a except for $\omega_{10}=-2.070$).

$$\dot{\omega}_2(t) = -a\,\dot{u}(t)\sin u(t); \qquad \dot{\omega}_3(t) = b\,\dot{u}(t)\cos u(t) \tag{12c, d}$$

When inserting these expressions in the Euler Eqs. (1b) and (1c) we obtain a surprisingly simple relationship between u and ω_1:

$$\dot{u}(t) + n_s\omega_1(t) = 0 \quad \text{with} \quad n_s = \sqrt{\frac{(B-A)(C-A)}{BC}} \tag{13a, b}$$

Thus, the variable u is proportional to the total turning angle $\int\omega_1(\tau)d\tau$ about the x-axis.

Eq. (13a) *is the key to an analytic solution in u*. First, it allows adopting u as the independent variable in Eq. (8):

$$\frac{d(\Delta E_{sep})}{du} = \frac{1}{n_s}\left(\frac{B-A}{B}\right)T_1 \;\Rightarrow \tag{14a}$$

$$\Delta E_{sep}(u) = \Delta E_{sep}(u_0) + \frac{1}{n_s}\left(\frac{B-A}{B}\right)T_1(u-u_0) \tag{14b}$$

The transition to a spin about the x-axis occurs at $\Delta E_{sep}=0$. When starting from a pure flat-spin motion about the z-axis, we find from Eq. **(7)**:

$$\Delta E_{sep,fs}(u_0) = \frac{C(C-B)}{2B}\omega_{30}^2 \quad \text{with:} \quad u_0 = \frac{\pi}{2} \tag{15a, b}$$

The linear relationship in Eq. (14b) has only one solution (see also Eq. (28b) of Ref. [13]), namely

$$u_{sep} = \frac{\pi}{2} - \frac{1}{2}\sqrt{\frac{C(C-A)}{B(B-A)}\frac{(C-B)}{T_1}}\omega_{30}^2 \tag{15c}$$

In order to investigate whether the value u_{sep} is reached or not, we insert the derivative of Eq. (13a) in the first Euler Eq. (1a). This produces a second-order differential equation for $u(t)$:

$$\ddot{u} - \frac{(C-B)\Delta E_0}{BC}\sin(2u) + n_s\frac{T_1}{A} = 0 \tag{16}$$

Eq. (16) has the structure of the forced nonlinear pendulum equation. For a flat-spin recovery, it is necessary that $\omega_1>0$ continues to increase. According to Eq. (13a), this implies that the solution $u(t)$ must continue to decrease and therefore an ongoing clockwise spin-up about the body's x-axis. When the solution in u is bounded, the pendulum is oscillating and there is no recovery. In this case, the motion is described by just a segment of the line $\Delta E_{sep}(u)$, see Ref. [13].

The first Euler Eq. (1a) gives now also the exact solution $\omega_1(u)$ and allows the derivation of the minimum torque level T_1^* that guarantees an unbounded solution for u and ω_1. These results have been derived in detail in Ref. [13] and are summarized as follows:

$$\omega_1^2(u) = \frac{\Omega_c^2}{n_s^2} - \frac{(C-B)\Delta E_0}{BCn_s^2}\cos(2u) - \frac{T_1}{An_s}(2u)$$

$$\omega_2(u) = a\,\cos u \tag{17a – c}$$

$$\omega_3(u) = b\,\sin u$$

with

$$\Omega_c^2 = n_s^2\omega_{10}^2 + \frac{1}{2}(n_i^2\omega_{20}^2 - n_t^2\omega_{30}^2) + 2n_s\frac{T_1}{A}u_0 \tag{17d}$$

$$n_s^2 = \frac{(B-A)(C-A)}{BC} \tag{17e}$$

$$n_t^2 = \frac{(C-B)(C-A)}{AB} \tag{17f}$$

$$n_i^2 = \frac{(C-B)(B-A)}{AC} \tag{17g}$$

The constant Ω_c^2 is a second integral of motion found by substituting Eqs. (12a)–(12d) in Eqs. (1).

Fig. 3 show two illustrative examples of a recovery under the indicated input data. If the torque ceases to act when $\omega_1=0$ we find from Eq. (7) that $\Delta E_{sep}=E_{sep}-E>0$ and, according to Eq. (6a), the resulting free motion is still a nutation about the z-axis. The transition to a spin about the x-axis occurs later at the crossing of $\Delta E_{sep}=0$, which corresponds to $u_{sep}=10.93^\circ$ $(<u_{\omega 1=0})$ when using Eq. (15c). We note that the derivative of $\omega_1(u)$ has a discontinuity at $\omega_1=0$, which may be avoided by using the quadratic formula in Eq. (17a).

Fig. 4 show the behavior when the torque T_1 approaches its critical value T_1^* for pure flat-spin initial conditions, i.e. $\omega_{10}=\omega_{20}=0$. Theoretically, the time to the transition (or the period of the periodic solution if there is no recovery) goes to infinity (i.e., there is no finite limit).

Please cite this article as: F.L. Janssens, J.C. van der Ha, Flat-spin recovery of spinning satellites by an equatorial torque, Acta Astronautica (2015), http://dx.doi.org/10.1016/j.actaastro.2015.05.011

The vertical lines in Fig. 4 identify specific points of interest, which are identified in Table 1.

The increase of these time intervals occurs with an enormous sensitivity as illustrated in Table 1. On the flat parts of the curves, the angular velocity is hardly moving at all in the body frame and is close to an unstable stationary solution. This remark is important for illustrating the continuity with the case $T_2 \neq 0$.

The main properties for a recovery when using a torque along the minimum axis are

i). depending on the magnitude of the torque, a nutation-type periodic spin-up/spin-down (see Fig. 4b) about the z-axis or a continuing recovery spin-up about the x-axis occurs;
ii). the transition to a spin-up about the x-axis can occur only during the first revolution of the angular velocity vector $\boldsymbol{\omega}$ with steadily decreasing nutation during this spin-up.

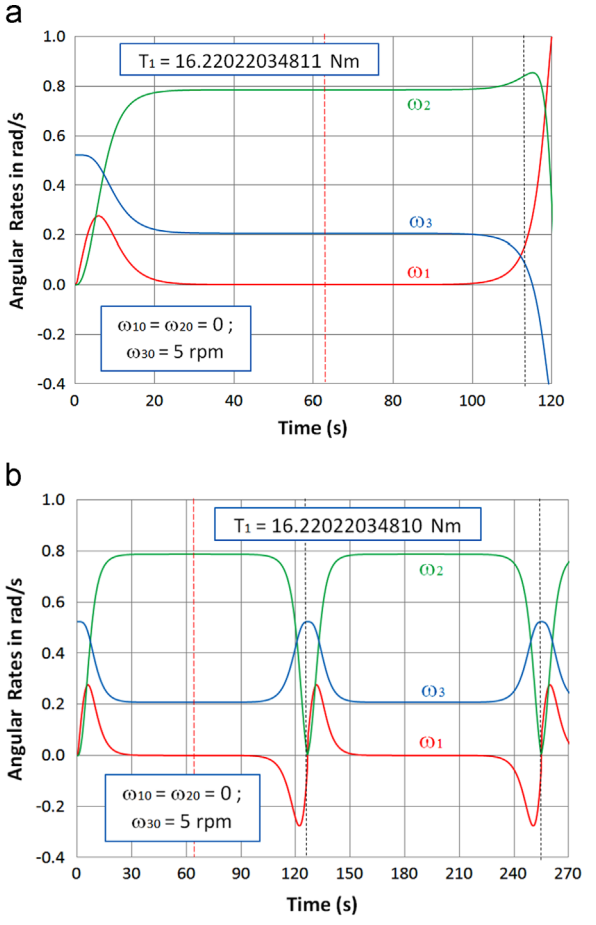

Fig. 4. (a) Angular rates $\omega_j(t)$, $j=1, 2, 3$, in case of recovery. (b) Angular rates $\omega_j(t)$, $j=1, 2, 3$, in case of no recovery.

4. Torque in x, y-plane

In the present section we consider a torque within the x, y-plane with components $T_1 > 0$, $T_2 \neq 0$. Eq. (10) indicates that the first integral ΔE_{max}=constant is no longer available now. The most important consequence is that, in this case, the transition does *not* need to occur within the first revolution after the onset of the torque.

Figs. 5 and 6 show a typical recovery for the case $T_2 = T \sin\alpha < 0$ with $\alpha = -5^\circ$ and $T = |\mathbf{T}| << T_1^*$, which is the critical value for a torque about the x-axis. It was shown in Refs. [15,16] that $T_2 < 0$ implies a secular decrease in ω_3 for an *asymmetric* body because the average value of ω_3 decreases under nutation. This dynamical mechanism leads to a transition followed by the spin-up about the minimum axis of inertia. At the start of the recovery maneuver the average decrease of ω_3 is slow. An approximate expression for the rate of decrease was derived based on the non-zero average value of the product $\omega_1\omega_2$ while assuming a constant ω_3 value (slowly varying parameter) during the nutation period:

$$\omega_3(t) \cong \omega_{30} \sqrt[3]{1+\frac{t}{\tau}} \tag{18a}$$

with

$$\tau = \frac{2}{3} \frac{C(C-A)(C-B)}{T^2(B-A)\sin(2\alpha)} \omega_{30}^3 \tag{18b}$$

The structure of Eqs. (18a) and (18b) suggests the following qualitative conclusions:

a) a spin-down occurs when $-\pi/2 < \alpha < 0$ for *any* value of the torque T;
b) the time to recovery goes to infinity when α approaches $-\pi/2$ or 0;
c) when $\alpha > 0$, Eqs. (18a) and (18b) predict a spin-up about z but the correct interpretation is that the critical torque T_1^* increases by an amount that depends on the value of α.

Fig. 7 shows the very slow spin-down of ω_3 during a longer timeframe. After the recovery, the behavior is comparable to the results observed [13] in the case $T_2 = 0$

Table 1
Summary of results near boundary between recovery and no recovery.

T_1 (Nm)	Result	$\Delta E_{sep}(t)=0$ at:	$\omega_1(t)$ (rad/s)
16.22022035	Recovery	95.649 s	Minimum 7×10^{-6} at 45.1 s
16.22022034811	Recovery	112.83 s	Minimum 1×10^{-6} at 62.7 s
16.22022034810	No recovery	–	$\omega_1=0$ at 61.5 s; Period is 126.5 s

Please cite this article as: F.L. Janssens, J.C. van der Ha, Flat-spin recovery of spinning satellites by an equatorial torque, Acta Astronautica (2015), http://dx.doi.org/10.1016/j.actaastro.2015.05.011

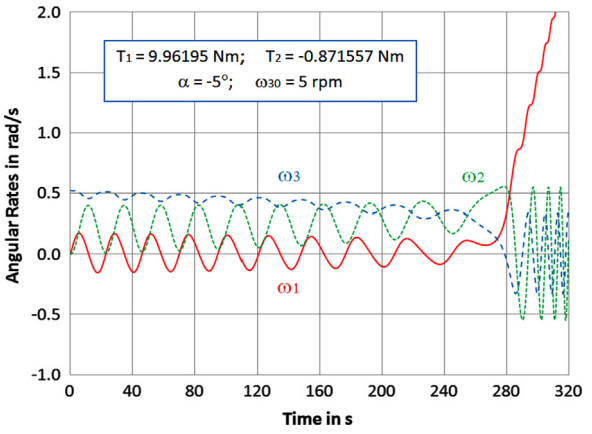

Fig. 5. Simulation Results for $|\mathbf{T}|=10$ Nm; azimuth angle $\alpha=-5^\circ$.

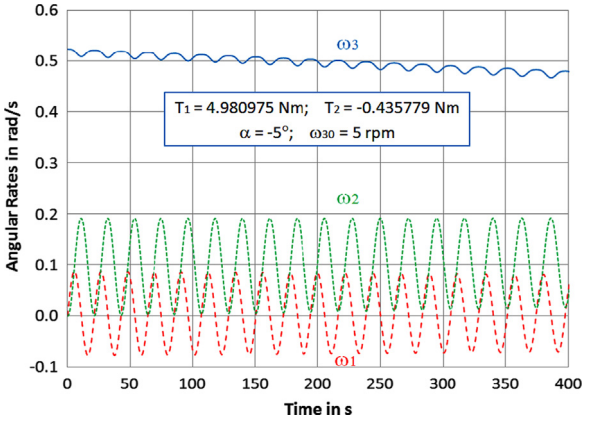

Fig. 6. Simulation Results for $|\mathbf{T}|=5$ Nm; azimuth angle $\alpha=-5^\circ$.

with adjusted average value of the angular velocity in the y, z-plane.

Eq. (13a) is instrumental for changing the independent variable from t to u. In this case, u keeps its meaning of total turning angle about the x-axis and starts from 0 (i.e., not at the pure flat-spin initial value $u_0=\pi/2$). The Euler equations (1) can now be written as (' denotes d/du):

$$-An_s\,\omega'_1\,\omega_1+(C-B)\omega_2\,\omega_3=T_1 \tag{19a}$$

$$-Bn_s\,\omega'_2\,\omega_1+(A-C)\omega_1\omega_3=T_2 \tag{19b}$$

$$-Cn_s\omega'_3+(B-A)\omega_2=0 \tag{19c}$$

After inserting Eq. (19c) in Eq. (19a) we find a total differential and hence the following new first integral:

$$k_1\omega_3^2-k_3\omega_1^2=k_1\omega_{30}^2+2k_3t_1u/n_s \tag{20a}$$

with

$$k_1=\frac{C-B}{A};\quad k_2=\frac{C-A}{B};\quad k_3=\frac{B-A}{C};\quad t_1=\frac{T_1}{A} \tag{20b-d}$$

Eq. (20a) represents a hyperbola with varying axes and is merely a different form of Eq. (14b).

Under this change of independent variable, the linear relationship in Eq. (14b) remains valid for $u_0=0$ and ΔE_{sep} $(u_{sep})=0$ (see also Eq. (15c)) and we have

$$u_{sep}=-\frac{1}{2}\sqrt{\frac{C(C-A)}{B(B-A)}\frac{(C-B)}{T_1}}\omega_{30}^2=-\frac{1}{2}\omega_{30}^2\frac{k_1}{t_1}\sqrt{\frac{k_2}{k_3}} \tag{21}$$

When inserting $u=u_{sep}$ from Eq. (21) in Eq. (20a) we obtain, as expected, $k_1\omega_{3,sep}^2=k_3\omega_{1,sep}^2$, which is the equation for the separation planes. Summarizing, we state that the existence of u_{sep} shows that a transition to a spin about the minimum axis always takes place when $T_1<0$ and $T_2>0$, which is a sufficient condition.

The second Euler equation shows that ω_2 is described by a harmonic oscillator, forced by ω_1:

$$\omega_2''+\omega_2=\frac{t_2}{n_s}\left(\frac{\omega_1'}{\omega_1^2}\right) \tag{22a}$$

with

$$t_2=\frac{T_2}{B} \tag{22b}$$

According to Eqs. (18a) and (18b) the minimum recovery time for a given $|\mathbf{T}|$ is in the vicinity of $\alpha=-45^\circ$. For $|\mathbf{T}|=10$ Nm, the azimuth angle of -39.5° gives the fastest recovery time t_{sep}.

Fig. 8a shows the angular velocity components for this case. The recovery time is $t_{sep}=68.68$ s and is indicated by the first dashed (red) vertical line. The respective ω_j ($j=1$, 2, 3) values at t_{sep} are 0.2436, 0.3319, 0.1722 rad/s, respectively. The second dashed (blue) vertical line in Fig. 8a is at $t=75.47$ s and corresponds to the first time that the ω_3 component reaches zero.

Fig. 8b shows the projection of the angular velocity in the y, z-plane. At the start, the value of ω_2 becomes slightly negative. When ω_3 goes negative, the trajectory appears to stabilize on an ellipse. *The continuation of the trajectory is comparable to the behavior observed in the case* $T_2=0$, see Ref. [13]. Fig. 8c shows the three-dimensional representation of the angular velocity components for the same case as in Fig. 8a and b.

Fig. 8d shows the behavior of ΔE_{max} (u). Initially, ΔE_{max} decreases from its starting value of 54.83 Nm but it eventually

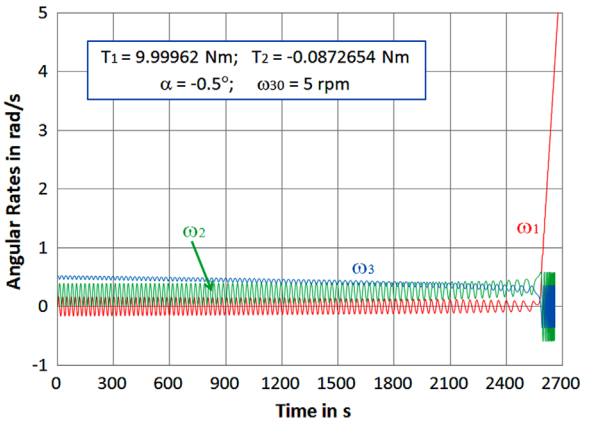

Fig. 7. Simulation Results for $|\mathbf{T}|=10$ Nm; $\alpha=-0.5^\circ$; $\Delta E_{sep}=0$ at $t=2581$ s.

Please cite this article as: F.L. Janssens, J.C. van der Ha, Flat-spin recovery of spinning satellites by an equatorial torque, Acta Astronautica (2015), http://dx.doi.org/10.1016/j.actaastro.2015.05.011

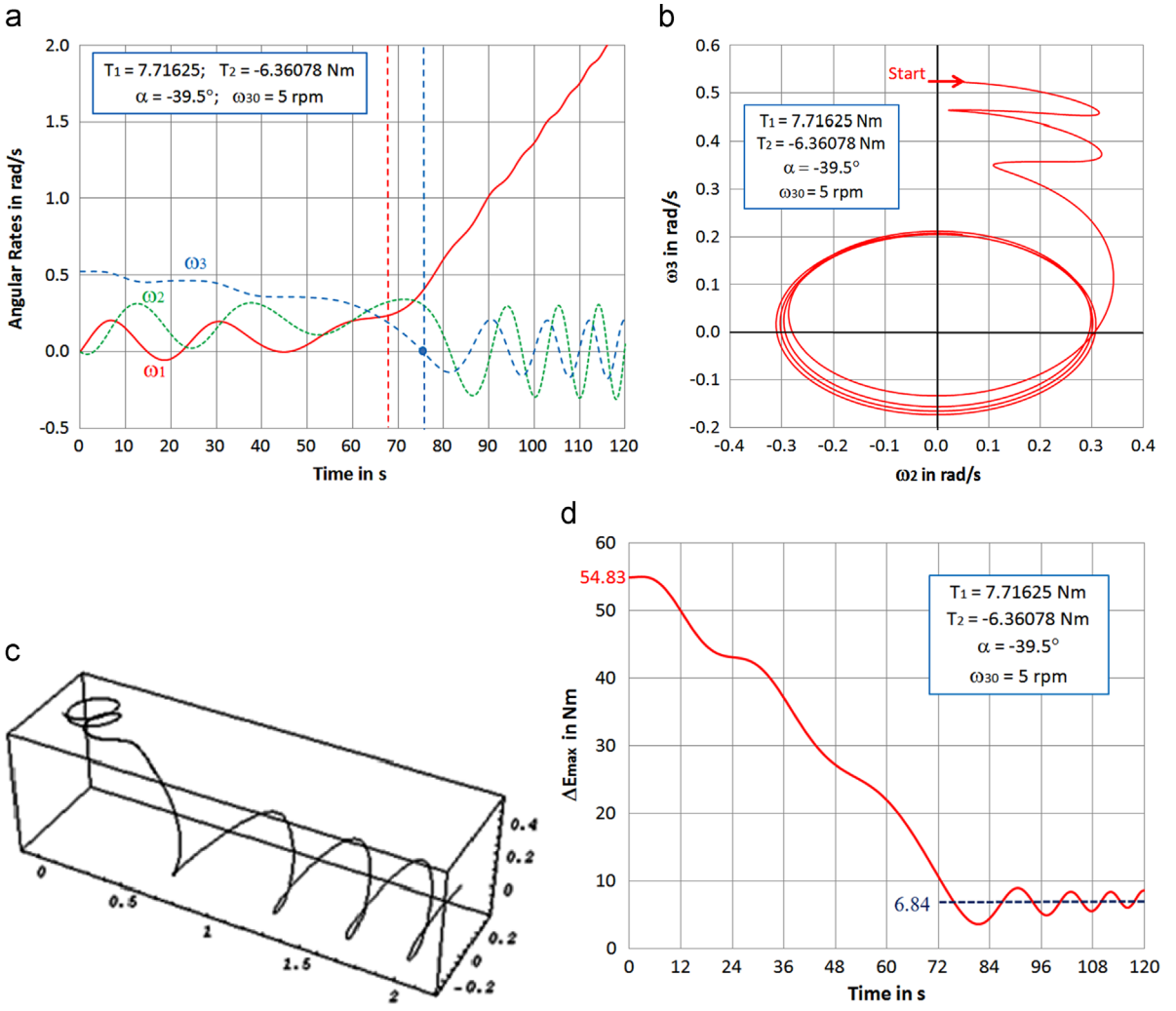

Fig. 8. (a) Results for $|\mathbf{T}|=10$ Nm; $\alpha_{opt}=-39.5^{\circ}$; (b) projection of $\boldsymbol{\omega}$ motion in y, z-plane. (c) 3-Dimensional illustration of vector $\boldsymbol{\omega}$; (d) evolution of ΔE_{max} to a constant value. (For interpretation of the references to color in this figure, the reader is referred to the web version of this article.)

stabilizes at about 6.84 Nm. In the case $t_2=0$ the term ΔE_{max} would have remained constant at 54.83 Nm throughout.

Finally, Table 2 provides a summary of the characteristic values related to the optimal direction angle α_{opt} for a few values of the torque magnitude. The results in Table 2 confirm that the magnitudes of equatorial torque vectors are indeed smaller than the corresponding minimum torque component (i.e., $T_1^*=16.22$ Nm) along the minimum inertia axis found in Ref. [13].

In summary, we conclude that a feasible flat-spin recovery can be constructed in the case when $T_1>0$ and $T_2<0$. For a given torque level we can optimize the azimuth angle α of the torque vector for the fastest possible recovery. The recovery time must be shorter than the time required for bringing the spacecraft in a flat spin through energy dissipation.

Table 2
Summary of simulation results as function of $|\mathbf{T}|$.

$\|\mathbf{T}\|$ (Nm)	α_{opt} (deg)	t_{sep} (s)	1st Time $\omega_3=0$ (s)	Final ΔE_{max} (Nm)
12	−36	43.5433	48.8119	10.5
10	−39.5	68.680	75.470	6.8
8	−41	113.710	123.096	2.4

5. Motion in inertial space

The motion of the body in inertial space has been investigated by means of numerical integrations. The inertial Z-axis is directed along the initial angular momentum vector $\mathbf{H}$ and the inertial X-axis is taken along the initial torque direction, which corresponds to the body x-axis in the pure flat-spin case. The inertial Y-axis completes the dextral system of axes. In this paper, small letters x, y, z refer to the principal body axes and capital letters X, Y, Z refer to the inertial axes.

First, we describe the results for two representative strategies aiming at recovery from a pure flat-spin situation. The inertias and initial flat-spin rate are as in the previous examples, i.e., $\omega_{10}=\omega_{20}=0$; $\omega_{30}=5$ rpm. Table 3

Please cite this article as: F.L. Janssens, J.C. van der Ha, Flat-spin recovery of spinning satellites by an equatorial torque, Acta Astronautica (2015), http://dx.doi.org/10.1016/j.actaastro.2015.05.011

Table 3
Torques and recovery times for two representative strategies.

Case	T_1 (Nm)	T_2 (Nm)	Time ($\Delta E_{sep}=0$) (s)	1st Time $\omega_3=0$ (s)
I. Torque along x-axis	16.2203	0	53.187	55.5266
II. Torque in x, y-plane	8 cos(−41°)	8 sin(−41°)	113.710	123.096

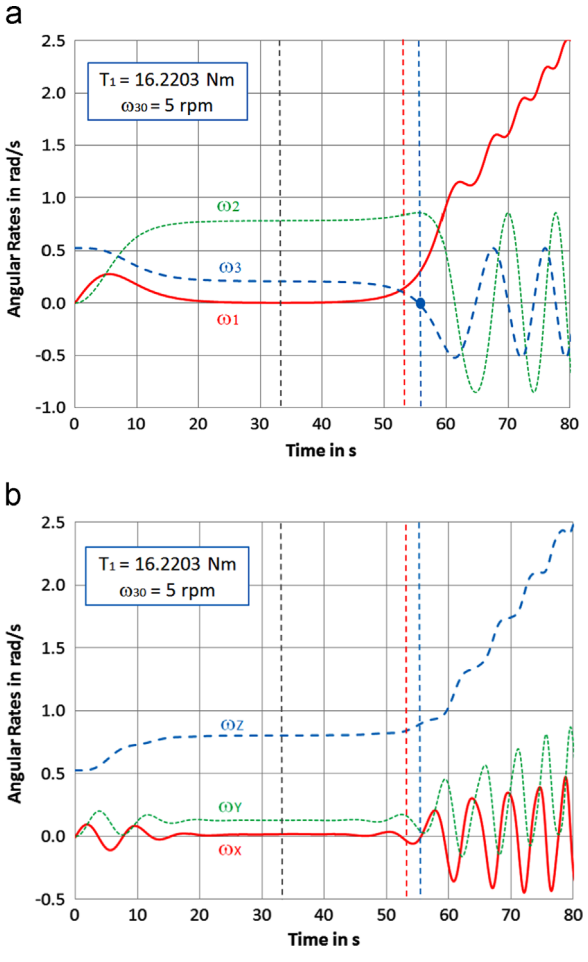

Fig. 9. (a) Angular velocities for $\omega_{30}>0$ in body frame. (b) Angular velocities for $\omega_{30}>0$ in inertial frame. (For interpretation of the references to color in this figure, the reader is referred to the web version of this article.)

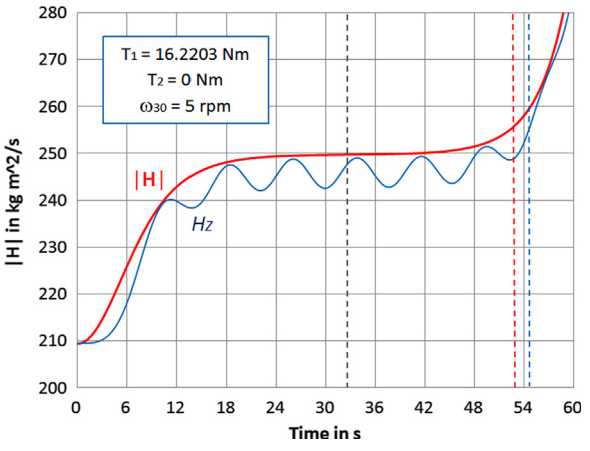

Fig. 10. Angular momentum |**H**| and H_Z.

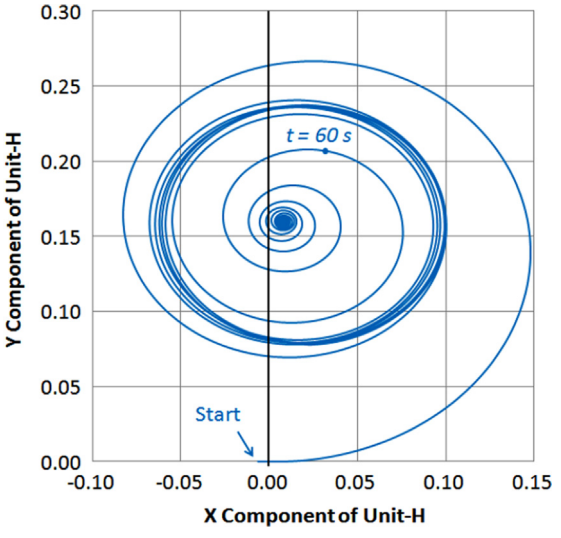

Fig. 11. Projection of unit-vector **H**/|**H**| on X, Y-plane.

summarizes the applied torques and corresponding recovery times.

5.1. Case I torque along x-axis

Figs. 9a and b shows the motion of the angular velocity components in the body frame and in the inertial frame, respectively. In the body frame (see Fig. 9a) the angular rate ω_1 reaches its minimum value at $t=32.9$ s, i.e. the first (gray) dashed vertical line. The transition occurs at $t_{sep}=53.2$ s, i.e. at the second (red) dashed vertical line. The rate ω_3 decreases from the start and crosses zero at $t=55.5$ s, i.e. the third (blue) dashed vertical line. Afterwards, it starts oscillating.

In the inertial frame (see Fig. 9b) the rate ω_Z keeps on increasing and, after the recovery, its behavior is comparable to ω_1 in Fig. 9a. The vertical lines are identical to those in Fig. 9a.

Fig. 10 shows the behavior of the modulus |**H**| of the angular momentum vector with initial value of 209.44 kg m^2/s along both the z and Z axes. Subsequently,

Please cite this article as: F.L. Janssens, J.C. van der Ha, Flat-spin recovery of spinning satellites by an equatorial torque, Acta Astronautica (2015), http://dx.doi.org/10.1016/j.actaastro.2015.05.011

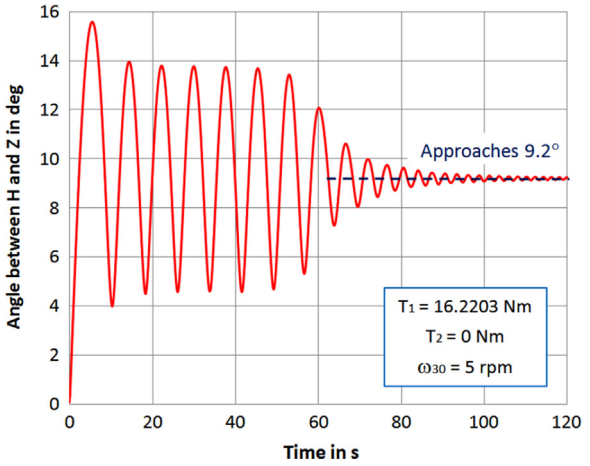

Fig. 12. Evolution of H-vector relative to inertial *Z*-axis.

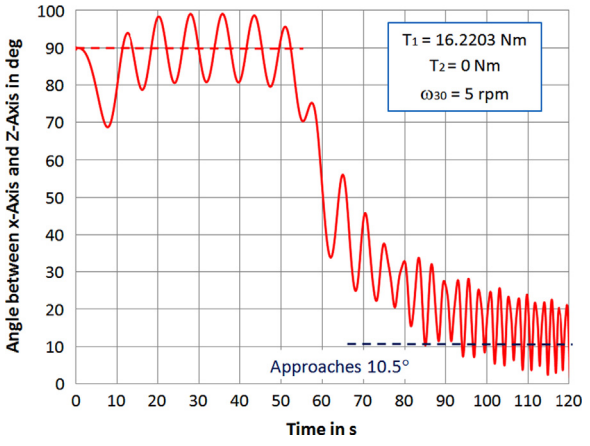

Fig. 13. Evolution of angle between *x*-axis and *Z*-axis.

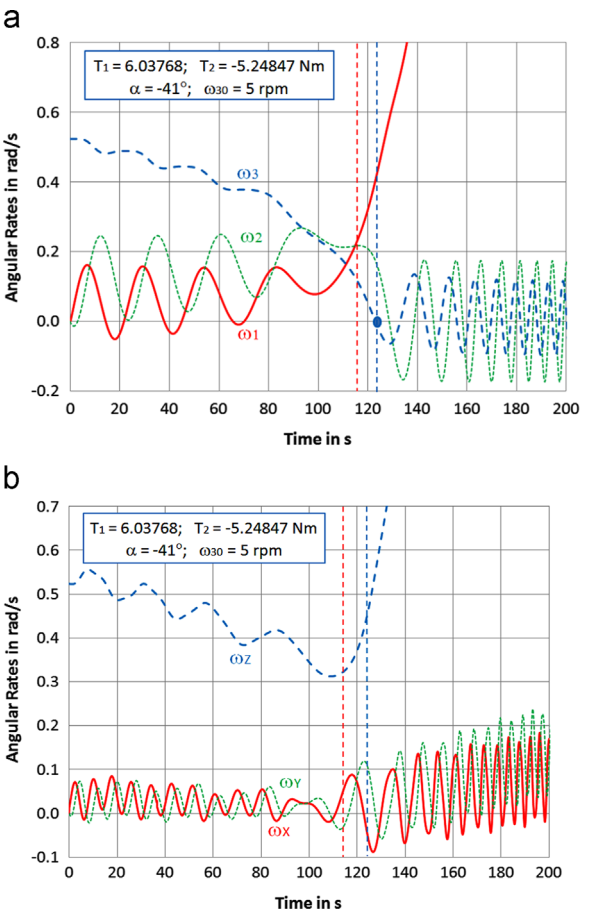

Fig. 14. (a) Angular velocity components in body frame. (b) Angular velocity components in inertial frame. (For interpretation of the references to color in this figure, the reader is referred to the web version of this article.)

it increases continuously while transferring the momentum to the *x*-axis. The component H_Z along the *Z*-axis follows with oscillations and the deviations of the vector **H** from the *Z*-axis remain relatively small. Again, the vertical lines are identical to those in Fig. 9a.

Fig. 11 shows the projection of the unit-vector $\mathbf{H}/|\mathbf{H}|$ on the *X*, *Y*-plane during the first 3 min of motion under the same inputs as used in Fig. 10. The transition occurs just before the 60-s mark shown in Fig. 11. Afterwards, the spin-up causes a decrease of the nutation and **H** converges towards a fixed direction. The final point of convergence is about 0.16 distance away from the origin, which corresponds to an offset angle of about 9.2°.

Fig. 12 shows the angle between the angular momentum vector and the *Z*-axis. During the first 50 s (i.e., before the transition) this angle shows oscillations with amplitudes of 4–5° about the limiting value of 9.2° as in Fig. 11. Afterwards, while nutating about the *x*-axis, the amplitude decreases fairly rapidly until it essentially dies out after about 2 min.

Fig. 13 illustrates the transfer of the angular momentum from the body *x*-axis to the inertial *Z*-axis, which starts after the transition at about 53 s and is completed about a minute later.

Figs. 10–13 provide informative insights on the recovery for the case $\omega_{30} > 0$ but we confirmed that the results for $\omega_{30} < 0$ are very similar. *Regardless of whether the flat spin is about the plus or minus body z-axis* (see Fig. 1), *a torque about the body +x-axis always restores the body x-axis in the neighborhood of the angular momentum vector* (*Z*) *before the onset of the dissipation* (*provided that the torque level exceeds a certain critical value*).

5.2. Case II torque in x, y-plane

Fig. 14 are the counterparts of Fig. 9. The torque level $|\mathbf{T}| = 8$ Nm is much smaller than the critical value $T_1^* = 16.22$ Nm in Case I and the torque direction angle for Case II is $\alpha = -41°$ (see Table 3). We observe the gradual decrease of ω_3 and ω_Z during several revolutions. As in Case I, the behavior of ω_Z after the recovery becomes comparable to that of ω_1. The dashed (red) vertical line at 113.71 s shows where the transition ($\Delta E_{sep} = 0$) occurs and the dashed (blue) line at 123.1 s is at the first zero crossing of ω_3.

Please cite this article as: F.L. Janssens, J.C. van der Ha, Flat-spin recovery of spinning satellites by an equatorial torque, Acta Astronautica (2015), http://dx.doi.org/10.1016/j.actaastro.2015.05.011

Fig. 15 shows that, after the recovery, the offset angle of the angular momentum vector with respect to the *Z*-axis decreases from about 17° and eventually stabilizes at about 4°. Fig. 15 also shows the convergence of the offset angle of the *x*-axis relative to the *Z*-axis to the same limiting value but at a much slower rate. The identical asymptotic offset angles for the *H*-vector and *x*-axis are induced by the decrease of the nutation.

Fig. 16 shows the projection of the unit-vector **H**/|**H**| in the *X*, *Y*-plane. It starts circling with an increasing radius about a center on the *Y*-axis until the recovery. Afterwards, it circles with a shrinking radius about a center at (−0.025, 0.058), which corresponds to an offset of about 3.6° from the *Z*-axis. The final offset angle is smaller than the 9.2° offset in Case I in Fig. 11.

Finally, we mention that a torque with a *positive* component along the *y*-axis must have a magnitude above the critical value to guarantee the flat-spin recovery. Its level depends on the positive offset angle α of the torque vector. Table 4 shows a few examples.

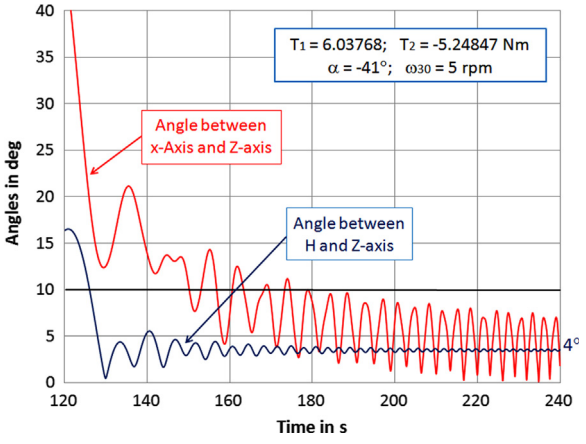

Fig. 15. Orientations of body *x*-axis and **H**-vector relative to Z-axis.

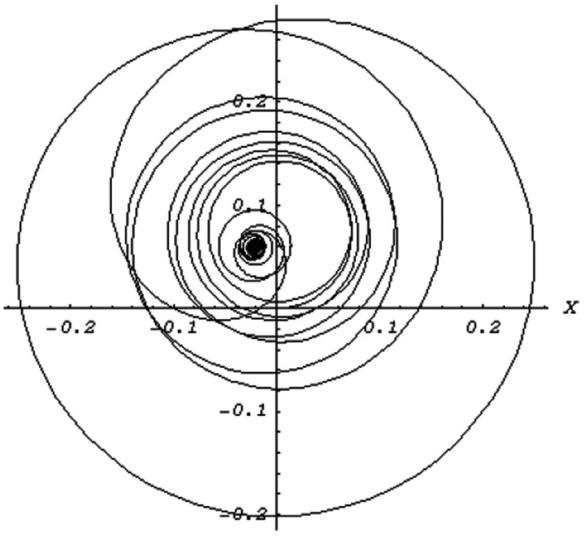

Fig. 16. Projection of unit-vector **H**/|**H**| on *X*, *Y*-plane.

Table 4
Examples of recovery/no recovery for positive α angles.

|T|	α (deg) for recovery	α (deg) for no recovery
16.25	0.1	0.25
16.30	0.5	0.70
16.50	1.5	2.0
18	10	13
20	18	20

5.3. Attitude matrix

The observed properties of the flat-spin recovery strongly advocate the use of the 1–2–1 rotation sequence [17] (see Fig. 17) because the results show that the first and second rotation angles, which define the orientation of the *x*-axis, stabilize asymptotically about a constant value. In addition, the third rotation accounts for the spin-up about the body *x*-axis. A first rotation $\varphi = 180°$ about *X* followed by a rotation $\theta = 90°$ about Y_1 brings the initial $x(=X)$-axis onto the *Z*-axis. These two rotation angles may then stabilize on the values $180° - \varepsilon_\varphi$ and $90° - \varepsilon_\theta$ where ε_φ and ε_θ designate small angles.

The attitude matrix [17] A^T corresponds to the 1–2–1 rotation sequence and maps a vector V_B from the body frame into the vector V_I within the inertial frame:

$$V_I = A^T V_B \tag{23a}$$

with

$$A^T = \begin{bmatrix} c\theta & s\theta s\psi & s\theta c\psi \\ s\theta s\varphi & -c\theta s\varphi s\psi + c\psi c\varphi & -c\theta s\varphi c\psi - s\psi c\varphi \\ -s\theta c\varphi & c\theta c\varphi s\psi + c\psi s\varphi & c\theta c\varphi c\psi - s\psi s\varphi \end{bmatrix} \tag{23b}$$

where *c* and *s* stand for the cosine and sine functions, respectively.

The inertial representation of the *x*-axis is

$$x_I = \begin{bmatrix} c\theta & s\theta s\varphi & -s\theta c\varphi \end{bmatrix}^T \tag{24}$$

This result contains only the rotation angles φ and θ while ψ is absent. The asymptotic orientation of the *x*-axis can now be expressed in the small deviation angles $\varepsilon_\varphi = \pi - \varphi$ and $\varepsilon_\theta = \pi/2 - \theta$:

$$x_I \cong \begin{bmatrix} \varepsilon_\theta & \varepsilon_\varphi & 1 \end{bmatrix}^T \tag{25}$$

In the following section we establish asymptotic values of ε_φ and ε_θ for t, $u_m \to \infty$ by means of an approximate model that replaces the later part (i.e., *after* the recovery) of the curves in Figs. 9–15. For the results of Case I (i.e., when the torque acts only along the *x*-axis) the model can be formulated in terms of Fresnel integrals. Fig. 8d indicates that this approximate model may also be adapted to Case II by introducing an appropriate constant value for ΔE_{max}.

Fig. 18 shows the evolution of the angles for Case I. Initially, the angle φ grows fast but then stabilizes on a value close to 7π after the recovery has been established (i.e., after crossing $\omega_3 = 0$ at 55.5 s, see Fig. 9a). Afterwards, the ongoing spin-up occurs in the increasing ψ angle. The

Please cite this article as: F.L. Janssens, J.C. van der Ha, Flat-spin recovery of spinning satellites by an equatorial torque, Acta Astronautica (2015), http://dx.doi.org/10.1016/j.actaastro.2015.05.011

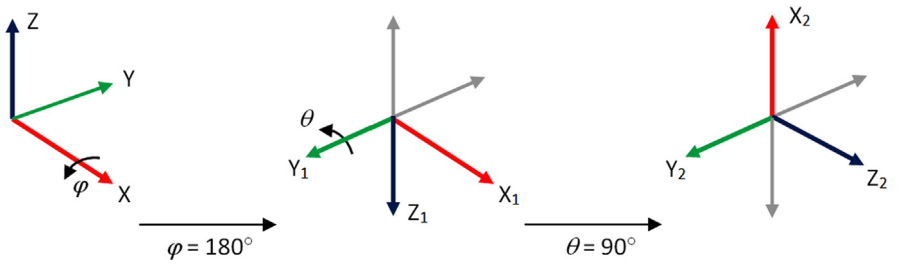

Fig. 17. The 1–2–1 sequence of rotations.

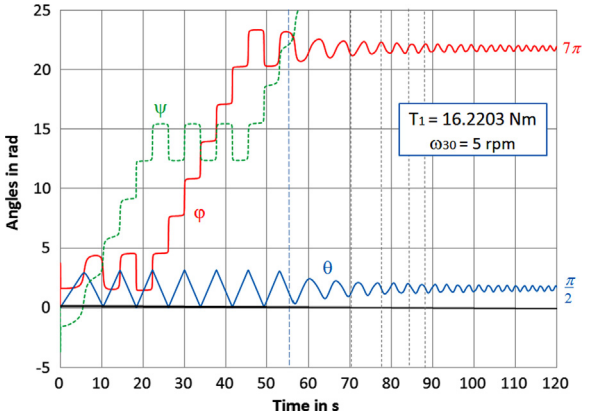

Fig. 18. Evolutions of angles φ, θ, and ψ for Case I (see Fig. 9a).

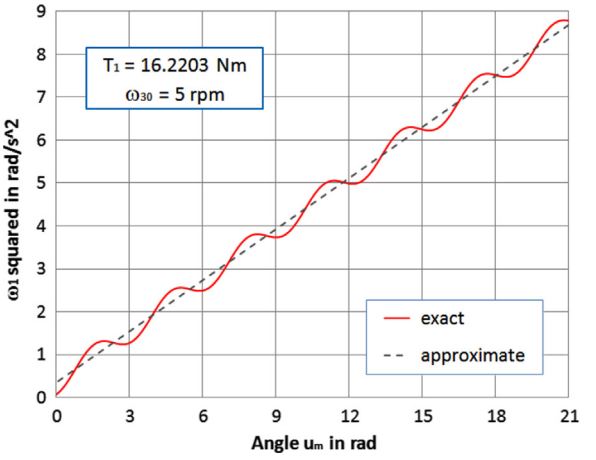

Fig. 19. Comparison of exact and approximate functions $\omega_1^2(u_m)$.

θ angle stays within the range $[0, \pi]$ and stabilizes on a value close to $\pi/2$. The dashed vertical lines in Fig. 18 indicate successive downwards passages of ω_3 through zero.

5.4. Asymptotic model for attitude angles

The derivation of the asymptotic values for the angles ε_φ and ε_θ makes use of the kinematic equations [17] based on the 1–2–1 sequence in Fig. 17. Furthermore, the independent variable u is replaced by $u_m = -u$ with $u = u(t)$ defined by its differential equation in Eq. (13a):

$$(\sin\theta)\,\dot{\varphi} = \omega_3 \cos\psi + \omega_2 \sin\psi \;\Rightarrow$$

$$(\sin\theta)\,\varphi' = \frac{1}{n_s\omega_1}(\omega_3 \cos\psi + \omega_2 \sin\psi) \tag{26a}$$

$$\dot{\theta} = -\omega_3 \sin\psi + \omega_2 \cos\psi \;\Rightarrow$$

$$\theta' = \frac{1}{n_s\omega_1}(-\omega_3 \sin\psi + \omega_2 \cos\psi) \tag{26b}$$

$$\dot{\psi} = \omega_1 - (\cos\theta)\,\dot{\varphi} \;\Rightarrow\; \psi' = \frac{1}{n_s} - (\cos\theta)\,\varphi' \tag{26c}$$

where $'$ denotes d/du_m and the analytical results for $\omega_j(u_m)$, $j = 1, 2, 3$, are given in Eqs. (17a)–(17c).

After the transition to the flat-spin recovery has taken place, the amplitudes a and b (of ω_2 and ω_3, respectively) may be replaced by their mean value $\langle\omega_{23}\rangle = \langle\omega_2^2+\omega_3^2\rangle^{1/2}$. Eqs. (26a) and (26b) may now be simplified as

$$(\sin\theta)\varphi' \cong \frac{\langle\omega_{23}\rangle}{n_s\omega_1(u_m)} \sin(\psi - u_m) \tag{27a}$$

$$\theta' \cong \frac{\langle\omega_{23}\rangle}{n_s\omega_1(u_m)} \cos(\psi - u_m) \tag{27b}$$

with

$$\langle\omega_{23}\rangle \cong \langle\omega_2^2+\omega_3^2\rangle^{1/2} = \left\{\frac{1}{2\pi}\int_{u_m}^{u_m+2\pi}[\omega_{23}^2(s)]\,ds\right\}^{1/2} = \sqrt{\frac{a^2+b^2}{2}} \tag{27c}$$

When starting from a pure flat-spin (i.e., $u_{m0} = -\pi/2$) Eq. (27c) becomes

$$\langle\omega_{23}\rangle_{pure\,fs} = \frac{\omega_{30}}{\sqrt{2}}\sqrt{1+\frac{C(C-A)}{B(B-A)}} = \frac{\omega_{30}}{\sqrt{2}}\sqrt{1+\frac{k_2}{k_3}} \tag{27d}$$

Thus, the ellipse described by ω_2 and ω_3 is now replaced by an approximate circular motion.

The second approximation is to replace the result for ω_1 in Eq. (17a) by

$$\omega_1(u_m) \cong \frac{1}{n_s}\sqrt{\Omega_c^2 + 2t_1 n_s u_m} \tag{28}$$

where the periodic term $\cos(2u_m)$, which averages to zero, has been neglected.

Fig. 19 shows that the approximate expression given in Eq. (28) may be acceptable for sufficiently large values of u_m. At the points $u_{m,k} = \pi/4 + k\pi/2$ (for $k = 0, 1, \ldots$) the

Please cite this article as: F.L. Janssens, J.C. van der Ha, Flat-spin recovery of spinning satellites by an equatorial torque, Acta Astronautica (2015), http://dx.doi.org/10.1016/j.actaastro.2015.05.011

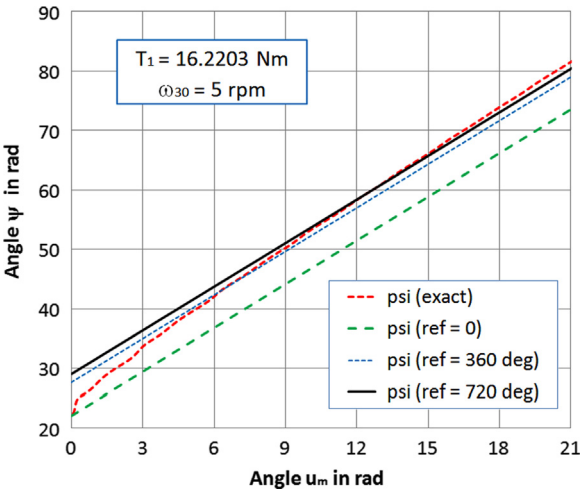

Fig. 20. Comparisons of linear approximations of angle $\psi(u_m)$.

approximation of Eq. (28) is exact. In general, however, the true $\omega_1(u_m)$ oscillates around the approximate value.

For values of u_m past the transition to a spin about the x-axis, the simulations show that Eq. (26c) may be adequately approximated by the linear relationship:

$$\psi(u_m) \cong \psi(u_{m,ref}) + \left(\frac{u_m - u_{m,ref}}{n_s}\right) = \tilde{\psi} + \frac{u_m}{n_s} \tag{29a}$$

with

$$\tilde{\psi} = \psi(u_{m,ref}) - \frac{u_{m,ref}}{n_s} \tag{29b}$$

Fig. 20 shows the comparisons of three linear approximations with different reference points (i.e., $u_{m,ref} = 0, 2\pi, 4\pi$) with the exact expression in Eq. (26c). We conclude that, as expected, the highest $u_{m,ref}$ (i.e., continuous black) line produces the most accurate approximation.

The approximation in Eqs. (29a) and (29b) is not obvious. When θ is near $\pi/2$ the cosθ term of Eq. (26c) is small. The term φ', however, is not small as ε_φ oscillates fast with small amplitude about $\pi - \text{mod}(\varphi, 2\pi)$. We note that the slopes of the approximations differ slightly from the slope of $\psi(u_m)$.

After incorporating all of these simplifications into Eqs. (26a) and (26b) we find a decoupled equation for $\theta(u)$. For θ near $\pi/2$ the equation for φ also decouples in first-order approximation so that

$$\theta'(u_m) = -\langle \omega_{23} \rangle \frac{\cos(\tilde{\psi} + c_k u_m)}{\sqrt{\Omega_c^2 + 2t_1 n_s u_m}} \tag{30a}$$

$$\varphi'(u_m) = -\langle \omega_{23} \rangle \frac{\sin(\tilde{\psi} + c_k u_m)}{\sqrt{\Omega_c^2 + 2t_1 n_s u_m}} \tag{30b}$$

with

$$c_k = \frac{1}{n_s} - 1 \tag{30c}$$

It is straightforward to write Eqs. (30a) and (30b) in terms of the small deviations $\varepsilon_\theta = \pi/2 - \theta$ and $\varepsilon_\varphi = \pi - \varphi$:

Table 5
Summary of Simulation Results for angles φ, θ, ψ at $u_m = 2k\pi$.

u_m (deg)	t (s)	φ (deg)	ε_φ (deg)	θ (deg)	ε_φ (deg)	ψ (deg)
0	55.55	247.5	−67.5	61.9	28.1	1270
360	69.95	151.6	28.4	55.4	34.6	2464
720	77.66	200.4	−20.4	87.9	2.1	3424
1080	83.69	151.0	29.0	105.0	−15.0	4357
1440	88.80	182.3	−2.3	70.7	19.3	5278
1800	93.33	164.6	15.4	108.4	−18.4	6192

$$\varepsilon'_\vartheta(u_m) \cong -\langle \omega_{23} \rangle \frac{\cos(\tilde{\psi} + c_k u_m)}{\sqrt{\Omega_c^2 + 2t_1 n_s u_m}} \tag{31a}$$

$$\varepsilon'_\varphi(u_m) \cong -\langle \omega_{23} \rangle \frac{\sin(\tilde{\psi} + c_k u_m)}{\sqrt{\Omega_c^2 + 2t_1 n_s u_m}} \tag{31b}$$

The solutions of the differential equations of the type in Eqs. (31a) and (31b) are expressed as follows:

$$\begin{aligned} \varepsilon_\theta(u_m) &\cong \varepsilon_{\vartheta,ref} - F\langle \omega_{23} \rangle \{ \cos d\,[C(z_m) - C(z_{ref})] \\ &\quad - \sin d\,[S(z_m) - S(z_{ref})] \} \\ \varepsilon_\varphi(u_m) &\cong \varepsilon_{\varphi,ref} - F\langle \omega_{23} \rangle \{ \cos d\,[S(z_m) - S(z_{ref})] \\ &\quad + \sin d\,[C(z_m) - C(z_{ref})] \} \end{aligned} \tag{32a, b}$$

where

$$C(x) = \int_0^x \left\{ \cos\left(\frac{\pi}{2} z^2\right) \right\} dz \tag{33a}$$

$$S(x) = \int_0^x \left\{ \sin\left(\frac{\pi}{2} z^2\right) \right\} dz \tag{33b}$$

are the Fresnel integrals with the arguments defined by

$$z_m = \sqrt{\frac{c_k}{\pi t_1 n_s}(\Omega_c^2 + 2t_1 n_s u_m)} \tag{34a}$$

$$z_{ref} = \sqrt{\frac{c_k}{\pi t_1 n_s}\left(\Omega_c^2 + 2t_1 n_s u_{m,ref}\right)} \tag{34b}$$

The remaining constants and coefficients appearing in Eq. (32a,b) are defined as follows:

$$F = \sqrt{\frac{\pi}{c_k t_1 n_s}} \tag{35a}$$

$$c = \cos d \tag{35b}$$

$$s = \sin d \tag{35c}$$

$$d = \tilde{\psi} - c_k \Omega_c^2 / (2t_1 n_s) \tag{35d}$$

By using the well-known [18] property that both $C(x)$ and $S(x) \to 0.5$ when $x \to \infty$, we obtain the asymptotic values $\varepsilon_{\theta,\infty}$ and $\varepsilon_{\varphi,\infty}$ from Eq. (32a,b) when substituting $z_m \to \infty$:

$$\begin{aligned} \varepsilon_{\theta,\infty} &\to \varepsilon_{\vartheta,\text{ref}} + F\langle \omega_{23} \rangle \{ C(z_{ref}) \cos d \\ &\quad - S(z_{ref}) \sin d - (\cos d - \sin d)/2 \} \end{aligned} \tag{36a}$$

$$\begin{aligned} \varepsilon_{\varphi,\infty} &\to \varepsilon_{\varphi,\text{ref}} + F\langle \omega_{23} \rangle \{ C(z_{ref}) \cos d \\ &\quad + S(z_{ref}) \sin d - (\cos d + \sin d)/2 \} \end{aligned} \tag{36b}$$

Please cite this article as: F.L. Janssens, J.C. van der Ha, Flat-spin recovery of spinning satellites by an equatorial torque, Acta Astronautica (2015), http://dx.doi.org/10.1016/j.actaastro.2015.05.011

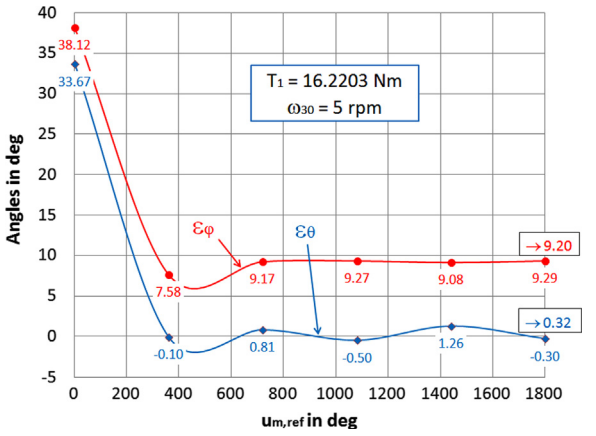

Fig. 21. Angular results from asymptotic model as function of $u_{m,ref}$.

5.5. Summary of numerical results

Table 5 summarizes the results for the angles φ, θ, ψ at the points $u_{m,k}=2k\pi$ obtained by numerical integration as in Fig. 18. Also the small deviation angles $\varepsilon_\varphi=\pi-\varphi$ and $\varepsilon_\theta=\pi/2-\theta$ are tabulated in Table 5. The separatrix is crossed at $t=53.2$ s, which is just *before* $u_m=0$ (see Fig. 9a). Thus, Table 5 contains only results from *after* the transition to a spin about the *x*-axis.

Table 5 provides the inputs for the asymptotic model in the previous section. Each of the u_m entries in the left column is used as a starting point (i.e., $u_{m,ref}$) for the integrated results of ε_φ and ε_θ in Eq. (32a,b). The associated initial conditions $\varepsilon_{\varphi,ref}$ and $\varepsilon_{\theta,ref}$ are also given in Table 5.

The resulting asymptotic values $\varepsilon_{\varphi,\infty}$ and $\varepsilon_{\theta,\infty}$ are given in Eqs. (36a) and (36b) and illustrated in Fig. 21. It can be seen that the asymptotic value $\varepsilon_{\varphi,\infty}$ remains steady from $u_{m,ref}=720^\circ$ onwards and converges to 9.2°, which agrees with the result shown in Fig. 12. Similarly, we find that the asymptotic value $\varepsilon_{\theta,\infty}$ converges to 0.32° but it keeps oscillating within a range of about 0.8°.

6. Conclusion

This paper studies the recovery from a flat-spin situation by means of a continuous torque in a plane perpendicular to the maximum axis of inertia. The main result is that, as long as the torque has a positive component along the desired spin axis (i.e., the *minimum* axis of inertia), a flat-spin recovery can always be achieved by a negative torque component along the intermediate axis. From previous work it is known that, for a torque aligned with the minimum inertia axis, there exists a critical minimum level that the torque must exceed in order to achieve a recovery. Here, a sufficient condition for recovery is established for a torque in the plane normal to the maximum inertia axis, namely that the torque component along the intermediate axis of inertia must be negative. There is no restriction on the torque's magnitude but the time to recovery increases indefinitely when this torque component approaches zero. For a given torque level, there exists an optimum orientation angle between the two torque components that minimizes the recovery time. During a recovery under this strategy, the angular momentum vector remains in the vicinity of its direction before starting the recovery. Finally, also a useful approximate model is presented that predicts the asymptotic deviation of the spin-axis attitude orientation in inertial coordinates. These new results have significant implications for the design of flat-spin recovery strategies for satellites that are required to be spinning about their minor axes of inertia.

References

[1] P.M. Barba, N. Furumoto, I.P. Leliakov, Techniques for flat-spin recovery of spinning satellites, in: Proceedings of the AIAA Guidance and Control Conference, Key Biscayne, FL, August 20–22, 1973, AIAA Paper 73-859.
[2] U.T. Bödewadt, Der Symmetrische Kreisel bei Zeitfester Drehkraft, Math. Z. 55 (1952) 310–320.
[3] R. Grammel, Die Stationären Bewegungen des Selbsterregten Kreisels und ihre Stabilität, Ing.-Arch. 21 (3) (1953) 149–156.
[4] R. Grammel, Der Selbsterregten Unsymmetrische Kreisel, Ing.-Arch. 22 (2) (1954) 73–97.
[5] E. Leimanis, The General Problem of the Motion of Coupled Rigid Bodies About a Fixed Point, Springer, New York, 1965.
[6] J.M. Longuski, P. Tsiotras, Analytical solutions for a spinning rigid body subject to time-varying body-fixed torques – Part I constant axial torques, Trans. ASME 60 (1993) 970–975.
[7] D.L. Cronin, Flat spin recovery of a rigid asymmetric spacecraft, J. Guid. Control 1 (4) (1978) 281–282.
[8] R. Livneh, B. Wie, New results for an asymmetric rigid body with constant body-fixed torques, J. Guid. Control Dyn. 20 (5) (1997) 873–881.
[9] R. Livneh, B. Wie, Asymmetric body spinning motion with energy dissipation and constant body-fixed torques, J. Guid. Control Dyn. 22 (2) (1999) 322–328.
[10] C.D. Rahn, P.M. Barba, Reorientation maneuver for spinning spacecraft, J. Guid. Control Dyn. 14 (4) (1991) 724–728.
[11] J.R. Gebman, D.L. Mingori, Perturbation solution for the flat spin recovery of a dual-spin spacecraft, AIAA J. 14 (7) (1976) 859–867.
[12] C.D. Hall, R.H. Rand, Spinup dynamics of axial dual-spin spacecraft, J. Guid. Control Dyn. 17 (1) (1994) 30–37.
[13] F.L. Janssens, J.C. van der Ha, Flat-spin recovery of spinning satellites by equatorial torque, in: Proceedings of the 24th AAS/AIAA Space Flight Mechanics Meeting, Santa Fe, NM, January 27–30, 2014, Paper AAS-14-453; Advances in the Astronautical Sciences, vol. 152, pp. 3495–3513.
[14] M. Kaplan, Modern Spacecraft Dynamics & Control Section 2.3.6, Wiley, New York, 1976.
[15] P. Boland, F. Janssens, The GEOS-1 dynamic experiment, ESA J. 3 (1979) 265–280.
[16] J.C. van der Ha, Perturbation solution of attitude motion under body-fixed torques, Acta Astronaut. 12 (10) (1985) 861–869.
[17] J. Wertz (Ed.), Spacecraft Attitude Determination and Control, Springer Scientific+Business Media, Berlin and New York, 1978, pp. 764–765.
[18] M. Abramowitz, I. Stegun, Handbook of Mathematical Functions, Dover, New York, 1970, 301.

Please cite this article as: F.L. Janssens, J.C. van der Ha, Flat-spin recovery of spinning satellites by an equatorial torque, Acta Astronautica (2015), http://dx.doi.org/10.1016/j.actaastro.2015.05.011